

Determination of the energy dissipation of a vortex in a superconductor using a giant magnetoresistive sensor

M. Pannetier-Lecoeur* and C. Fermon†

CAPMAG/DRECAM/DSM, CEA Saclay, 91 191 Gif-sur-Yvette, France

(Received 21 September 2005; published 4 November 2005)

We present a method to determine the dissipation energy of a controlled number of vortices flowing in a superconductor. The principle is to use a mixed sensor made of a large superconducting loop closed by a micron-size constriction coupled to a giant magnetoresistive sensor. The results obtained on niobium are in good agreement with the heat-transfer model developed in this report, which allows to determine accurately the dissipation energy of a vortex.

DOI: [10.1103/PhysRevB.72.180501](https://doi.org/10.1103/PhysRevB.72.180501)

PACS number(s): 74.25.Qt, 75.47.De, 85.25.Am

The energy dissipation of a vortex, when it flows in a superconductor, is an essential parameter which controls superconductor transport properties.¹ A large number of publications report the determination of this dissipation energy in various stable regimes of vortices flow by transport measurement,^{2,3} susceptibility,⁴ noise measurements,^{5,6} or mechanical measurements.⁷ One spectacular phenomenon is the apparition of unstable regimes, such as flux jumps and avalanches, when the dissipated energy is larger than the heat transfer. A flux jump is a thermomagnetic instability where the motion of vortices in a superconductor leads to a sudden increase of temperature, which can induce, by an avalanche-like phenomenon, a local transition to the normal state. Flux jumps and vortex avalanches have been extensively studied theoretically^{8,9} and experimentally^{10–14} during the past years in conventional and high- T_c superconductors. However, the energy dissipated by a vortex is very difficult to measure in these regimes since the heat propagates very fast in superconductors and creates a nonlocal problem.

We have recently developed magnetometers, called mixed sensors, able to measure magnetic fields in the femtotesla range.¹⁵ The main idea of the mixed sensors is to use a micron-size magnetic sensor for the measurement of a current circulating in a superconducting loop. The loop is made of a large ring closed by a small constriction. If a magnetic field is applied perpendicular to this ring, a supercurrent appears to prevent the entrance of the magnetic flux in the loop. This effect is limited by the critical current in the small constriction. When the field is increased over this limit, the supercurrent is still limited to its critical value and some flux can enter in the loop. The entrance is done by vortices crossing the point of the loop where the critical current density is firstly reached, i.e., the constriction. The number of crossing vortices and their flow are accurately controlled by the applied magnetic field.

If the vortex flow is big enough, the dissipated energy is sufficient to warm locally the constriction until the transition temperature of the constriction is reached; this is a local flux jump. The magnetic sensor allows us to monitor the evolution of the supercurrent as a function of time and applied field.

In this Communication, we first present the device, fol-

lowed by the experimental curves corresponding to flux jumps and their statistics. Finally, we deduce the energy dissipated by the vortices when crossing the constriction using a diffusion model and we explain the dispersion of energy necessary to warm the constriction.

The device comprises a superconducting niobium loop deposited on top of an isolated giant magnetoresistance (GMR) sensor (see Fig. 1). The resistance of the GMR varies as a function of the in-plane magnetic field. Conventional photolithography techniques are used to pattern the device. Details of the fabrication process are given elsewhere.¹⁵

The device's loop has an external diameter of 25 mm and an internal diameter of 15 mm. It contains a constriction 6- μm wide and 20- μm long. The experiment is performed at 4.2 K with the sample placed in an anticyrostat under a small pressure of ⁴He to facilitate thermal exchanges.

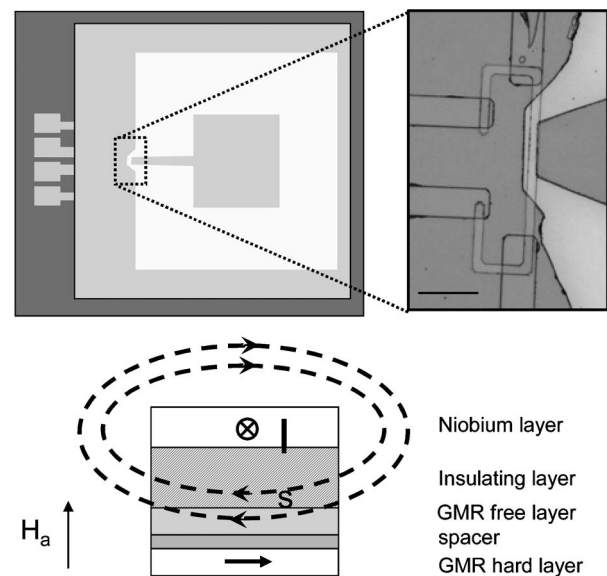


FIG. 1. Schematic view of the device (left-hand side). The constriction aligned with the yoke-type sensor is shown on the micrograph (right). The full stack for the niobium device is represented in the bottom part. The field lines generated in the constriction by the screening supercurrent I_s act on the rotation of the GMR-free layer.

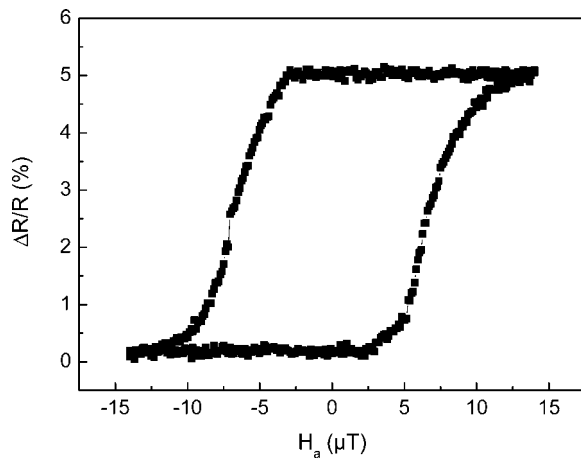


FIG. 2. Voltage variation in the MR for an applied field of $-15/+15 \mu\text{T}/-15 \mu\text{T}$ scanned on 500 points. The corresponding field step is $0.12 \mu\text{T}$.

The magnetoresistance as a function of a perpendicular magnetic field at 4.2 K is given in Fig. 2. The performance of this mixed sensor is related to the quality of the GMR stack, as well as to the geometry of the loop. To have the highest enhancement of the applied field, in the vicinity of the constriction, the loop should have a large diameter (a few millimeters at least), with a rather wide surface,¹⁶ and the constriction should be as small as possible to increase the local superconducting current density. The enhancement factor between the local in-plane field measured by the sensor at the constriction location, and the applied field, calculated from the geometry and the size of the sensor, is 516.

When applying a perpendicular field to the device at a temperature below T_c , the magnetoresistance increases to the upper plateau, which corresponds to the point where the supercurrent reaches its critical value. The same phenomenon occurs when switching down the field to a negative value. The maximum slope for the resistance change obtained in this device is of $961\%/m\text{T}$, compared to the in-plane field slope of $2.13\%/m\text{T}$, leading to an enhancement factor of 451 compared to the applied field. The critical current density can be calculated from the field experienced by the sensor and its geometry.¹⁷ We obtain a critical current density of $2 \times 10^6 \text{ A/cm}^2$ at 4.2 K. When the magnetoresistance reaches the maximal value which corresponds to the critical current in the constriction, a sufficiently high and fast increase of the magnetic field induces a transition to the normal state in the constriction which destroys the supercurrent; this effect is detected by a sudden drop of the GMR resistance. After the resistance drops, the constriction returns to the superconducting state. If the field is further increased the same effect can occur again. The same phenomenon has been observed on smaller size samples.

As shown in Fig. 3, during a cycling of the applied field, drops occur several times, always followed by an increase of the MR to the saturation. If the MR curve is not perfectly centered, the height of the drop can be different on the upper and lower plateau.

An important parameter in the occurrence and frequency of the drops is the slope of the applied field. This aspect has

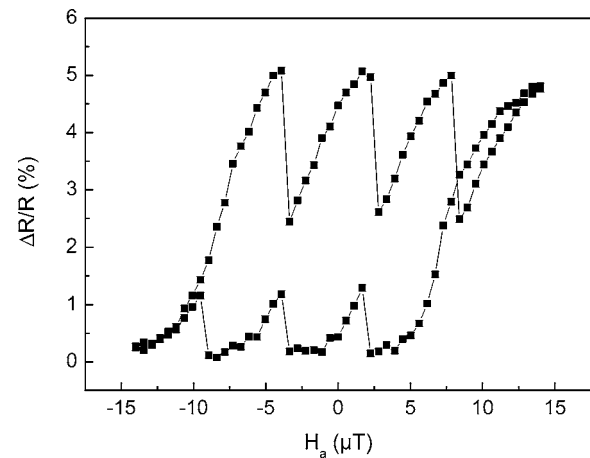


FIG. 3. Voltage variation in the MR for an applied field of $-15/+15 \mu\text{T}/-15 \mu\text{T}$ scanned on 100 points. The corresponding field step is $0.6 \mu\text{T}$.

been studied by changing the height of the field steps. The duration of the steps, monitored by a GHz oscilloscope, is 500 ns, independent of the step height.

The sensor response as a function of the applied field is given for the same field range ($\pm 15 \mu\text{T}$) but at two different numbers of steps (500 and 100) in Figs. 2 and 3. For the lowest number of steps (Fig. 3), there is a drop every time the critical current in the constriction is reached. In contrast, for a higher number of steps (smaller field slope) in the scanning process (Fig. 2), no drops occur on the whole curve.

Figure 4 shows the number of drops for $+10/-10 \mu\text{T}$ field cycles, as a function of the field step height. Each point represents results averaged on at least ten cycles.

It clearly appears that for steps smaller than $0.15 \mu\text{T}$ (equivalent to a field sweep rate below 0.3 T/s), the system is stable and no drop occurs. In the range of $0.15-0.45 \mu\text{T}$ ($0.3-0.9 \text{ T/s}$), the number of drops increases roughly linearly with the field step height, and then reaches a plateau corresponding to the maximum number of drops possible within a cycle, taking into account the field necessary to

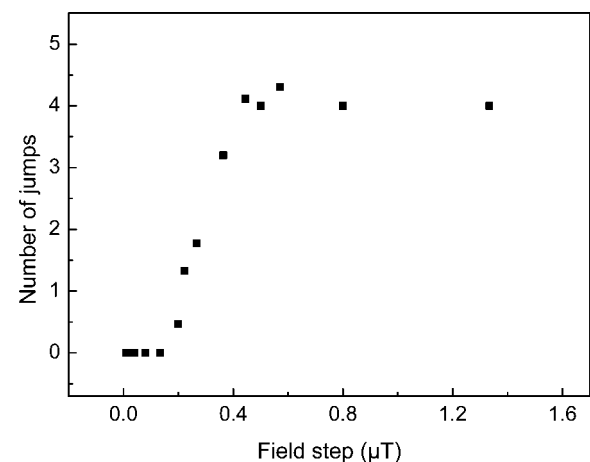


FIG. 4. Number of jumps as a function of the field step applied to the sample for the Nb—B device. The field has been scanned between -10 and $+10 \mu\text{T}$ at a different rate.

reach the critical state again. For higher values, the number of drops increases to reach its maximum value, given by the total applied field divided by the field required to reach the plateau.

When the critical current is reached, an additional field step induces vortices to enter the loop through the constriction, while the large part of the loop, due to its size, remains mainly in the Meissner state. Each vortex crossing the constriction leads to a dissipation of energy. A drop of the supercurrent implies that somewhere in the constriction, the temperature has reached the critical temperature of the constriction, 6.5 K (Ref. 18). For a 0.15- μT step, 7 250 vortices (0.15 μT over the loop surface, 100 mm^2) should cross the constriction. In this case, the corresponding dissipated energy is three times smaller than for a 0.45- μT step.

In order to understand this dispersion of energy we have modeled the temperature behavior when the vortices cross the constriction. The heat diffusion equation as a function of temperature T and position r is given by

$$C(r,T)\frac{\partial T}{\partial t} = \lambda(r,T)\Delta T - (T - T_0)h/d + P(r,t),$$

where C is the heat capacity, λ is the heat conductivity, h is the heat-transfer coefficient at the interface, d the thickness of the Niobium, and P is the power brought by the motion of vortices in the constriction. The heat capacity per unit volume is temperature dependent and varies as $C(T) = 40.3T + 29.3T^3 \text{ JK}^{-1} \text{ m}^{-3}$ (Ref. 19), leading to $C = 2340 \text{ JK}^{-1} \text{ m}^{-3}$ at 4.2 K. The heat conductivity depends on the quality of the niobium and varies with temperature as $T^{2.5}$ (Ref. 20). From the variation of resistivity from room temperature to low temperature of our sample, we obtain that $\lambda(T) = 0.11T^{2.5}$.

Outside of the constriction, the niobium is directly in contact with the substrate. We have experimentally determined²¹ a value of h for our sample to be $5 \times 10^4 \text{ Wm}^{-2} \text{ K}$. Inside the constriction, that value is reduced due to the insulator and the GMR barriers. From the number of interfaces and the quality of the insulator, we can estimate that the heat-transfer coefficient is equal to $1.2 \times 10^4 \text{ Wm}^{-2} \text{ K}$.

We have investigated various scenarios for the possible locations of the vortices when crossing the constriction, and compared them with the hypothesis of a uniform and homogeneous flow through its whole width. We identify two limit cases in terms of the energy dissipated. In the first case, all the vortices pass through a single channel. With a certain amount of energy, the temperature increase is sufficient to reach the critical temperature of the constriction (6.5 K). In the second case, vortices cross through two different paths located on the edges of the constriction, and thereby in contact with the large area of the main loop part. In this case, and with the same amount of energy, the temperature does not locally reach T_c ; the main loop acts as a thermal reservoir. This is the case requiring the highest energy for a flux jump. In the case where a homogeneous distribution of the vortices is considered, the temperature rise is higher than in the second case, but not sufficient (Fig. 5). Thus the energy required for a local transition of the constriction is dependent of the path followed by the vortices.

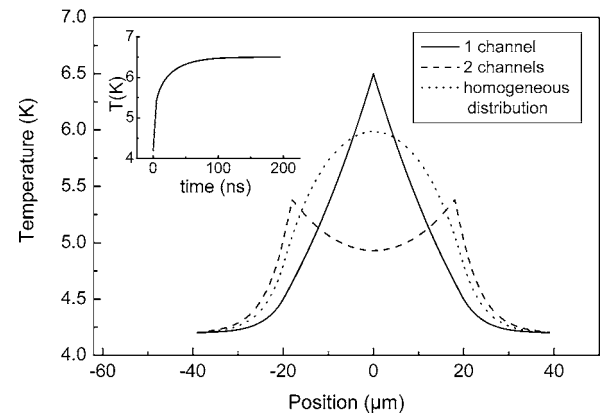


FIG. 5. Temperature distribution in the constriction obtained from a heat diffusion model, for a dissipated energy of $2.15 \times 10^{-12} \text{ J}$, when the vortices cross the constriction on a single channel centered (plain line), when the vortices cross along two different channels located at the edges of the constriction (dashed line), and when the vortices are homogeneously distributed along the constriction (dotted line). The inset shows the increase of temperature as a function of time.

In the most favorable case, with a single central path, the required energy, $E_1 = 2.15 \times 10^{-12} \text{ J}$, is 2.9 times lower than in the least favorable case ($E_2 = 6.2 \times 10^{-12} \text{ J}$), when the vortices channel on the edge and the heat is dissipated mainly in the large loop. When a field step larger than 0.45 μT is applied, whatever the vortices' path, the energy dissipated is always sufficient to warm the constriction above its critical temperature, giving a jump probability of 1. The energy dispersion given by our model is in good agreement with the experimental data (Fig. 4), where the probability of jumps varies from 0 to 1 between E_{\min} (0.15 μT) and $3E_{\min}$ (0.45 μT). From our results, we know that the probability to warm the constriction at a temperature higher than 6.5 K is nonzero when more than 7 250 vortices (0.15 μT of extra field applied to the inner surface of the loop) passes within 500 ns of the field ramping time. We can then deduce that the energy dissipated by each crossing vortex is about $2.96 \times 10^{-16} \text{ J}$ for a 5- μm path, i.e., $5.93 \times 10^{-11} \text{ J m}^{-1}$.

It is also important to note that the simulation predicts a constant value for the maximum temperature after only 50 ns. This implies that if the experiment time is larger than 50 ns, the good parameter for the stability of the constriction is not the total number of vortices but the number of vortices per second. We can give a critical speed of $3 \times 10^{10} \text{ vortex/s}$, corresponding to a speed of 0.3 T/s on the main loop. This value is comparable with the field sweep rates of flux-jump observations.⁵

However, one can note a fundamental difference between our approach and flux jumps observed in macroscopic systems where, for example, a decrease of flux jumps is observed with the increase of the sweeping rate.²² In our system, the transition phenomenon is rather different from the magnetothermal instabilities and flux jumps as described by Mints,²³ for example, since our system is not unstable and the oscillating behavior is given only by the fact that we need

to reach the critical current before a drop. The dispersion of energy, and therefore the probability of drops observed, are only created by the multitude of possible paths for vortices due to the length of the constriction.

In conclusion, the specific configuration of mixed sensors has allowed us to precisely control the crossing of vortices through the constriction. We have measured the energy dis-

sipated per vortex in the case where a vortex flow is created with a very small external applied magnetic field and in the presence of a well-known flowing current.

The authors would like to thank M. Viret and P. Lecoeur for fruitful discussions. They are grateful to R. J. Wijngaarden for useful suggestions.

*Author to whom correspondence should be addressed. Email address: mpannetier@cea.fr

†Email address: cfermon@cea.fr

¹N. B. Kopnin, Rep. Prog. Phys. **65**, 1633 (2002).

²Y. Ando *et al.*, Phys. Rev. B **47**, 5481 (1993).

³D. P. Norton and D. H. Lowndes, Phys. Rev. B **48**, 6460 (1993).

⁴O. Festin, P. Svedlindh, F. Rönning, and D. Winkler, Phys. Rev. B **70**, 024511 (2004).

⁵A. T. Fiory *et al.*, Appl. Phys. Lett. **52**, 2165 (1988).

⁶J. Houlrik, A. Jonsson, and P. Minnhagen, Phys. Rev. B **50**, 3953 (1994).

⁷S. Gregory *et al.*, Phys. Rev. Lett. **62**, 1548 (1989).

⁸R. G. Mints and L. Rakhmanov, Rev. Mod. Phys. **53**, 551 (1981).

⁹R. G. Mints and E. H. Brandt, Phys. Rev. B **54**, 12421 (1996).

¹⁰P. Leiderer, J. Boneberg, P. Brüll, V. Bujok, and S. Herminghaus, Phys. Rev. Lett. **71**, 2646 (1993).

¹¹L. Legrand, I. Rosenman, R. G. Mints, G. Collin, and E. Janod, Europhys. Lett. **34**, 287 (1996).

¹²E. Altshuler and T. H. Johansen, Rev. Mod. Phys. **76**, 471 (2004), and references therein.

¹³M. S. Welling, M. R. J. Westerwaal, W. Lohstroh, and R. J. Wijn-

gaarden, Physica C **411**, 11 (2004).

¹⁴I. S. Aranson *et al.*, Phys. Rev. Lett. **94**, 037002 (2005).

¹⁵M. Pannetier, C. Fermon, G. Legoff, J. Simola, and E. Kerr, Science **304**, 1648 (2004).

¹⁶M. Pannetier, C. Fermon, G. Legoff, and E. Kerr, in Proceedings of the European Magnetic Sensors and Actuators (EMSA), Cardiff (UK), July 2004, to be published in Sens. Actuators B.

¹⁷M. Pannetier, C. Fermon, G. Legoff, J. Simola, E. Kerr, M. Welling, and R. J. Wijngaarden, IEEE Transactions on Applied Superconductivity, **15**(2), Pt. 1, pp. 892–855, June 2005.

¹⁸The critical current is given by the magnetoresistance. At the transition temperature, the resistance does not change any more. The critical temperature can be therefore easily determined.

¹⁹C. Chou *et al.*, Phys. Rev. **109**, 788 (1958).

²⁰F. Koechlin and B. Bonin, Supercond. Sci. Technol. **9**(6), 453 (1996).

²¹With a current in the GMR, we send a known power and we monitor the temperature by the variation of the Niobium critical current.

²²D. Monier and L. Fruchter, Eur. Phys. J. B **3**, 143 (1998).

²³R. G. Mints, Phys. Rev. B **53**, 12311 (1996).